

Evaluating the Performance of Algorithms in Estimating the Chl-a Concentration of Lake Bafa

Elif Kirtiloglu*¹, Hakan Karabork²

¹Konya Technical University, Graduate Education Institute, Konya, Turkiye

²Konya Technical University, Faculty of Engineering and Natural Sciences, Geomatic Engineering, Konya, Turkiye

Keywords

Chlorophyll-a
Inland water bodies
Cyanobacteria
Water quality
Sentinel 2
Remote Sensing

ABSTRACT

Monitoring and estimating pigment concentrations in water bodies have a critical role in early intervention or investigation of causes for prevention. Remote sensing data are the most effective alternative due to its advantages as effortless, requiring less labor, and displaying large areas in a single frame. Analyzing and estimating Chlorophyll-a (Chl-a) concentrations constitute the most important research topics in water bodies because all phytoplankton contain Chl-a. In this study, we evaluated the performance of algorithms in estimating the Chl-a concentration of Lake Bafa based on Sentinel 2 bands which are simulated from in-situ reflectance data. We used 1/R665xR705, 1/R665-1/R705, (1/R665-1/R705) x R740, R705/(R560+R665), so called M09, G09-2B, G09-3B, K07, respectively and Normalized Difference Chlorophyll Index (NDCI) algorithms for evaluation. Water samples and in-situ measurements were collected and obtained in two field campaigns. Bands of Sentinel 2 were then simulated from in-situ reflectance data and used to calibrate and validate models for Chl-a estimation. R² values of 0.679, 0.749, 0.395, 0.726, and RMSE values of 0.7 and 1.882, 1.663, 1.737, and 1.818 µg/L have been obtained for M09, G09-2B, G09-3B, K07, and NDCI algorithms, respectively. Sentinel 2 images have been used for map validation. Our results show that M09 and NDCI algorithms performed better in estimating Chl-a compared to the other three algorithms for our data range at Lake Bafa.

1. INTRODUCTION

The estimations of biologists showed that the total biomass of phytoplankton is less than one billion tones in the ocean at any one time. It is less than 1% when compared to all photosynthetic biomass compared to earth plants with a total biomass of 500 billion tons (Falkowski, 2012). However, they are responsible for nearly 50% of global net primary production and are the primary energy source for aquatic ecosystems (Field et al., 1998), and are also of global significance for climate regulation and biogeochemical cycling. All water bodies on Earth contain high numbers of phytoplankton groups which have a great impact on also ecosystem change (Mishra et al., 2013). Cyanobacteria are a variety of bacteria that are included in this group and are the most common species (Ruiz-Verdú et al., 2008) and it is undesirable to increase in lake ecosystems (Mishra et al., 2013). It poses a major threat to water bodies (Paerl et al., 2011).

Although gathering information about their densities and distributions supports risk assessment and management activities (Hunter et al., 2009) and it is also highly associated with monitoring and evaluation of water quality (Shi et al., 2014). Several studies have been conducted using remote sensing techniques as an emerging tool in the inland and coastal waters to monitor the phenomenon of the cyanobacterial blooms focusing on a temperate reservoir (Beck et al., 2017), optically complex waters like oceans (Soja-Wo et al., 2017), turbid productive waters (Mishra et al., 2013), inland and near-coastal waters (Matthews & Odermatt, 2015), and inland waters (Kudela et al., 2015). These studies investigate the presence of Chlorophyll-a (Chl-a) and Phycocyanin (PC) pigments for the monitoring and detection of cyanobacteria (Hunter et al., 2010). Different sensors have used in different studies and appropriate algorithms (Gitelson et al., 2009; Koponen et al., 2007; Mishra & Mishra, 2012; Moses et al., 2019) were developed by considering the cost, temporal, spatial, and spectral resolution. In

* Corresponding Author

(elifkiyak@gmail.com) ORCID ID 0000-0002-8449-2588
(hkarabork@ktun.edu.tr) ORCID ID 0000-0001-7387-7004
Received: xx/xx/xxxx; Accepted: xx/xx/xxxx

parallel to technological developments, sensor technologies will provide optimum solutions for the monitoring of cyanobacteria. Analyzing and estimating Chl-a concentrations constitute the most important research topics in water bodies, because all phytoplankton contain Chl-a. To estimate the volume of phytoplankton and biomass, the Chl-a concentration can be used as an indicator (Vinh et al., 2019).

Many lakes in Turkey are under the influence of increasing population, climate change, agriculture and many anthropogenic activities and events. Lake Bafa, the largest lake in the Aegean region and the 15th largest in Turkey, is also under the negative influence of these factors. The main sources of income in the region surrounding the lake are tourism, fishing, animal husbandry and agriculture.

Because of the first Chl-a estimation algorithms have been developed for marine waters (adapted for blue and green regions of electromagnetic spectrum), they are inappropriate for inland waters as it was mentioned in Watanabe et al., (2018). The main reason is that the high colored dissolved organic matter (CDOM) masks the Chl-a absorption. In addition to this, inland waters such as rivers, reservoirs or lakes need higher spatial resolution sensors considering their size. Landsat and MERIS had the most suitable sensors, but they are no longer available today. The other options like Sentinel 2 (S2) should be considered as an alternative.

The main goal of this research was to evaluate the performance of algorithms in estimating the Chl-a concentration of Lake Bafa based on S2 bands which are simulated from in-situ reflectance data. We used $1/R665 \times R705$, $1/R665 - 1/R705$, $(1/R665 - 1/R705) \times R740$, $R705/(R560 + R665)$, so called M09, G09-2B, G09-3B, K07 respectively in this paper and Normalized Difference Chlorophyll Index (NDCI) algorithms. Water samples and in-situ measurements collected in two field campaigns. Bands of S2 were simulated from in-situ reflectance data and used to calibrate and validate models for Chl-a estimation.

2. MATERIALS AND METHODS

2.1. Study Area

Lake Bafa is an alluvial barrier lake, and it is in the Büyük Menderes River Basin. This basin is one of the largest basins of Turkey and is located within the borders of the Aegean region – the western part of the country. The lake lies between $37^{\circ}20' - 37^{\circ}34' N$ latitudes and $27^{\circ}22' - 27^{\circ}33' E$ longitudes. It is surrounded by the Beşparmak Mountains to the north and east, the İlbir Mountains to the south, and the fertile alluvial plains of the Büyük Menderes Delta to the west (Figure 1).

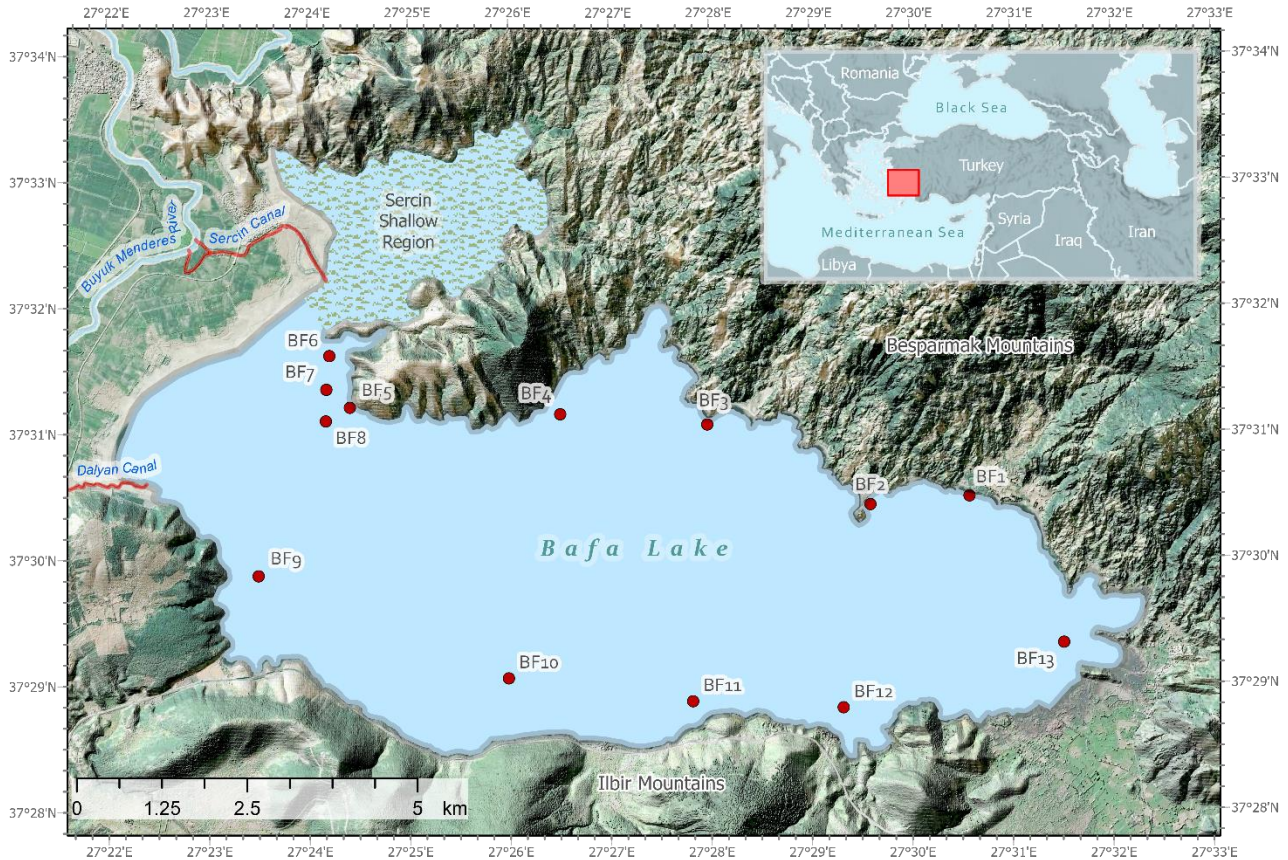


Figure 1. Study area and distribution of in-situ data sample stations in Lake Bafa

The area of the lake is about 6.708 hectares, and its depth varies between 0.5m and 25m. The lake is fed by rains, groundwater, small streams from the mountains, and the Büyük Menderes River. The Turkish General Directorate of State Hydraulic Works (DSI) controls the water level with hydraulic barriers. Water inlets and outlets are controlled by the regulators in the Dalyan and Serçin regions.

2.2. In-situ data

Two field studies were carried out as two campaigns on 17 July 2018 and 10 September 2019 and water samples collected at 13 fixed stations (labelled as BF1–BF13 in Figure 1). Water samples and corresponding remote sensing reflectance values were tried to be collected from the homogeneously distributed points from the lake surface. Since the Northwest part of the lake (Serçin shallow area, shaded area in Figure 1) is very shallow, the region could not be reached with watercraft and water samples could not be collected.

A total of 26 water samples were collected in this study. They were collected from the lake surface from < 50cm deep and stored in 1-liter sterile plastic bottles, and kept in a cold and dark isolated box until conducting pigment absorption and concentration measurements in the laboratory analyzes for Chl-a. The sum of Chl-a was determined with a spectrophotometer after extraction with hot ethanol (10260 ISO, 1992).

2.3. Calibration of Empirical Models

We evaluated models (empirical algorithms, Table 1) using S2 bands and simulated in-situ reflectance data that was used to calibrate and validate models for Chl-a estimation.

Table 1. Investigated empirical algorithms

Short Name	Algorithms	Reference
M09	$R_{665}^{-1} \times R_{705}$	(Moses et al., 2019)
G09_2B	$R_{665}^{-1} - R_{705}^{-1}$	(Gitelson et al., 2009)
G09_3B	$(R_{665}^{-1} - R_{705}^{-1}) \times R_{740}$	(Gitelson et al., 2009)
K07	$R_{705}/(R_{560} + R_{665})$	(Koponen et al., 2007)
NDCI	$(R_{705} - R_{665}) / (R_{705} + R_{665})$	(Mishra & Mishra, 2012)

¹ https://sentinels.copernicus.eu/web/sentinel/user-guides/sentinel-2-msi/document-library/-/asset_publisher/Wk0TKajlSaR/content/sentinel-2a-spectral-responses

² <https://scihub.copernicus.eu/>

In-situ remote sensing reflectance spectra was convoluted Sentinel 2 bands using S2 Spectral Response Functions (S2-SRF) v3.0¹.

2.4. Sentinel 2 Data, Image Processing and Chlorophyll-a Mapping

Sentinel-2 Level-1C (L1C) images were downloaded from Copernicus Open Access Hub² for the period of 2018–2019 years. The L1C images are 100x100km ortho images of Top of Atmosphere (TOA) and projected to UTM Zone 35N projection and WGS 1984 datum.

Downloaded images were processed with the ACOLITE³ atmospheric correction processor. The ACOLITE is a generic processor developed at RBINS for atmospheric correction and processing for coastal and inland water applications. It performs the atmospheric correction by default using the Dark Spectrum Fitting approach.

Images were reprojected to geographic coordinate system with WGS 1984 datum by the Sentinel Application Platform (SNAP)⁴ which is developed by Brockmann Consult, SkyWatch, and C-S, a free open toolbox for processing data from the Sentinel missions. Furthermore, SNAP was used for pixel calculation and preparing Chl-a distribution maps.

Although in-situ measurement was planned for the S2 MSI overpass date, the image of 17 July 2018 was under the influence of high sun glint. Thus 19 July 2018, and 10 September 2019 S2 images were used for algorithm validation. There was a cyanobacterium bloom on 24 June 2018, therefore the S2 image of this date was used for map validation.

2.5. Validation

6 of the 20 collected samples were used for validation of the empirical models. The used statistical metrics were the Mean Square Error (MSE, Eq. 1); Root Mean Square Error (RMSE, Eq. 2); Normalized Root Mean Square Error (NRMSE, Eq. 3) Mean Absolute Percentage Error (MAPE, Eq. 4) and determination coefficients (R²).

$$MSE = \frac{1}{n} \sum_{i=1}^n (y_a - y_p)^2 \quad (1)$$

$$RMSE = \sqrt{\frac{1}{n} \sum_{i=1}^n (y_a - y_p)^2} \quad (2)$$

$$\%NRMSE = \left(\frac{RMSE}{y_{max} - y_{min}} \right) * 100 \quad (3)$$

³ <https://odnature.naturalsciences.be/remsem/software-and-data/acolite>

⁴ <https://step.esa.int/main/toolboxes/snap/>

$$MAPE = \frac{1}{n} \sum_{i=1}^n \left| \frac{(y_a - y_p)}{y_a} \right| * 100 \quad (4)$$

Where, y_{max} is the maximum measured value; y_{min} is the minimum measured value; y_p are predicted values; y_a are measured values, and n is the number of samples.

3. RESULTS AND DISCUSSION

3.1. Laboratory Analysis

The values of the laboratory measurements of Chl-a and measured basic water quality parameters summary statistics are (PH, water temperature, dissolved oxygen) shown in Figure 2 and Table 2. According to analysis results, the Chl-a concentration varies between 4.04 and 8.51 $\mu\text{g/L}$ with a minimum value of 4.04 $\mu\text{g/L}$ at the BF10 station and with maximum values of 8.51 and 8.02 $\mu\text{g/L}$ at the BF8 and BF6 stations respectively.

It can be noticed that the June 2018 data has higher values for all parameters compared to September 2019.

When the Chl-a values were examined, the maximum value was 8.51 ($\mu\text{g/L}$). In fact, an algal bloom was observed in the Lake in June 2018, however, a sample could not be taken during the algal bloom due to the short duration and the

difficulty in obtaining measurement and transportation vehicles rapidly. However, Bafa is a productive lake, and it is possible to reach studies in the literature obtained previous Chl-a values ranging from 0.18 to 200 ($\mu\text{g/L}$) as 0.2 - 200.0 $\mu\text{g/L}$ from Hepsogutlu (2012), 0.2 - 200.0 $\mu\text{g/L}$ from Kesici (2015), 13.6 $\mu\text{g/L}$ from Kızılkaya et al., (2016), 0.73 - 32.44 $\mu\text{g/L}$ from Kocak (2017), and 0.18 - 3.88 $\mu\text{g/L}$ from Ozturk (2018).

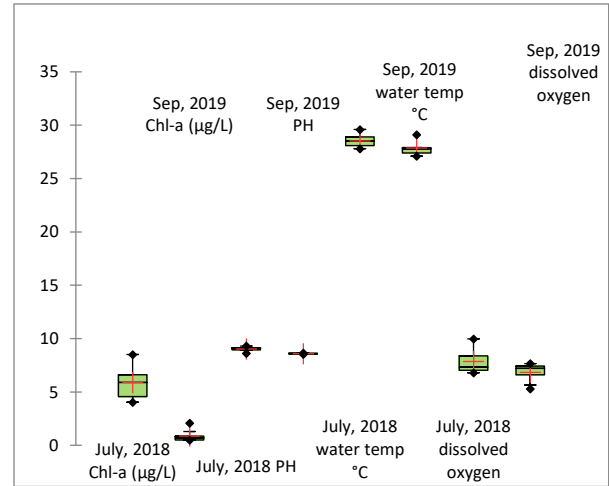


Figure 2. Results of the laboratory analyzes and water quality parameters

Table 2. Summary statistics of the laboratory analyzes and water quality parameters

Statistic	July 2018 Chl-a ($\mu\text{g/L}$)	Sep 2019 Chl-a ($\mu\text{g/L}$)	July 2018 PH	Sep 2019 PH	July 2018 water temp $^{\circ}\text{C}$	Sep, 2019 water temp $^{\circ}\text{C}$	July 2018 dissolved oxygen	Sep, 2019 dissolved oxygen
Minimum	4.040	0.500	8.620	8.530	27.800	27.100	6.800	5.280
Maximum	8.510	2.080	9.300	8.650	29.600	29.100	9.970	7.650
Mean	5.879	0.875	9.042	8.586	28.538	27.885	7.854	6.850
Standard deviation ($n-1$)	1.373	0.518	0.178	0.037	0.571	0.697	1.105	0.761

ASD-FS4 Hi-Res spectroradiometer⁵ which has 350-2500 nm wavelength range and 1 nm spectral resolution was used to acquire the in-situ spectral response. A total of 20 reflectance spectra were collected from two campaigns and 13 stations. We couldn't obtain reflectance spectra from 6 stations due to the battery problem of watercraft that have been occurred as an unexpected error during operation. The reflectance values were measured by following Mobley (1999) protocols early hour in the morning and with a clear sky. The surface reflectance measurements were collected from 10-15 cm above the surface and averaged for each cite (Figure 3). ViewSpec Pro software⁶ 5.6 was used for processing.

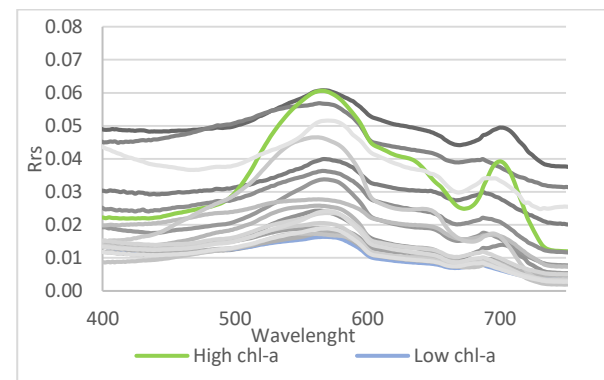


Figure 3. Spectral reflectance averages for 20 measurements.

⁵ <https://www.malvernpanalytical.com>

⁶ <https://www.malvernpanalytical.com/en/support/product-support/software/viewspecprosoftwareinstall>

3.2. Chl-a Algorithms

The performance of the five main algorithms used in the literature in Lake Bafa is summarized in the Table 3 and regression graphics in Figure 4.

It should be noticed that the tested models had been evaluated with low relatively narrow and low Chl-a values. Low RMSE values and high %NRMSE values were obtained as expected due to the

character of the data set. A significant correlation in all models has been obtained. G09_2B has the highest R^2 value and the fewest error results as M09, G09_2B, K07, NDCI have close R^2 values with 0.679, 0.749, 0.726, 0.700 and RMSE values with 1.882, 1.663, 1.737, 1.818 respectively. The G09_3B model has lower R^2 and higher RMSE values compared to the other four models.

Table 3. Performances of selected Chl-a estimation algorithms

Model	R^2	MSE	RMSE	%NRMSE	MAPE	Empirical Chl-a Algorithm
M09	0.679	3.543	1.882	23.498	123.528	$y = 16.061x - 10.348$
G09_2B	0.749	2.764	1.663	20.755	130.9	$y = 0.0959x + 6.0894$
G09_3B	0.395	6.664	2.581	32.227	174.148	$y = 24.88x + 5.4482$
K07	0.726	3.017	1.737	21.686	108.926	$y = 32.682x - 6.6527$
NDCI	0.7	3.307	1.818	22.701	119.679	$y = 30.778x + 6.0008$

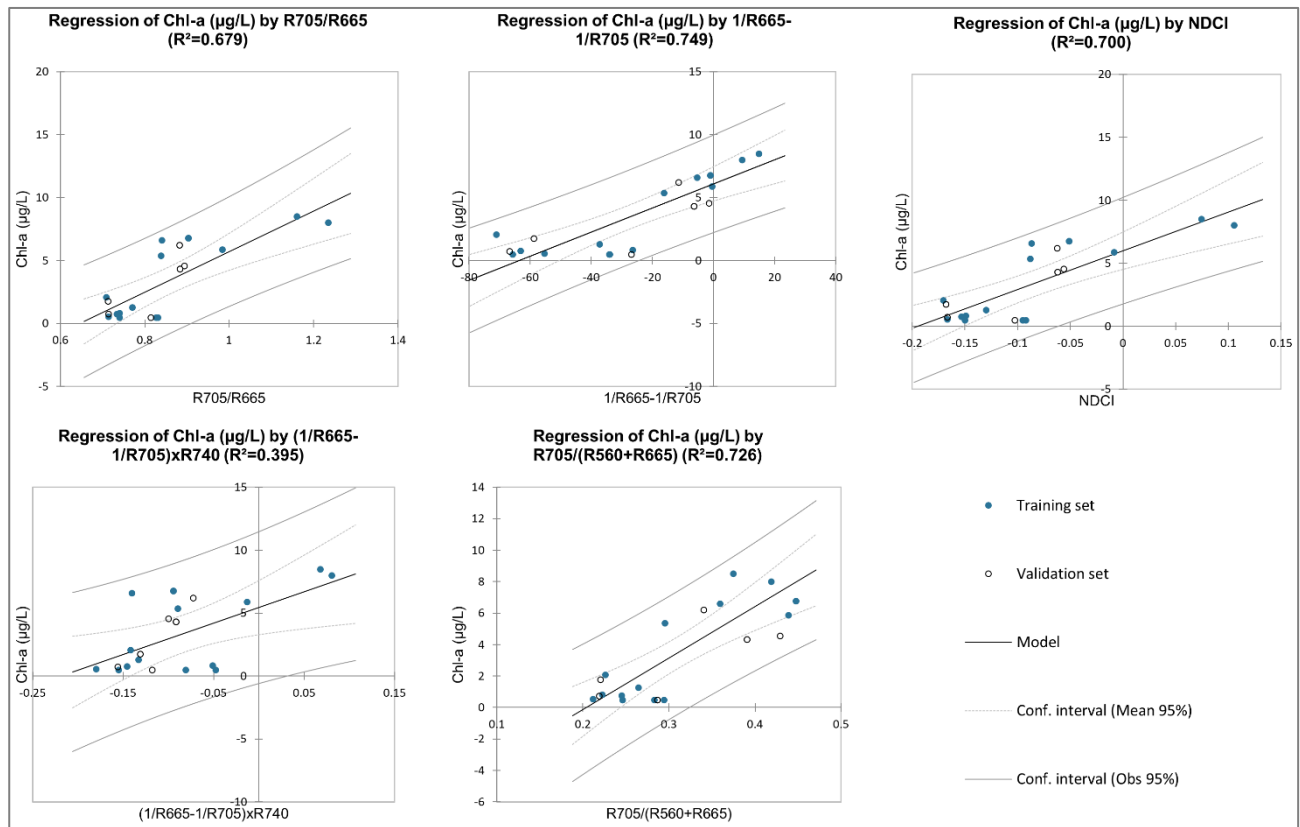


Figure 4. Regression graphics of the five main algorithms used in the literature in Lake Bafa.

3.3. Map Validation

We applied the selected algorithms to S2 images to evaluate the applicable range, performance, and validity. The three selected S2 images for map validation were: 19 July 2018, 10 September 2019 and 24 June 2018. First campaign was planned on 17 July 2018 during the S2 overpass, but since the same day S2 image was exposed to the sun glint effect, the

S2 image dated 19 July 2018, which covers 50% of the lake was used in the validation.

The distribution of the Chl-a values calculated by the models for the stations and the in-situ Chl-a values are given in Figure 5. As it can be seen from the figure that, all models are successful in predicting the Chl-a trend. To interpret the models and Chl-a estimations, it is necessary to compare the calculated trend for the model with the in-situ Chl-a estimation trend. The vertical axis represents the amount of Chl-

a in $\mu\text{g/L}$ unit, while the horizontal one shows station names. So, it is clear from the Figure 5 that, the predictions of BF10 and BF13 stations gave the least accuracies. All models were underestimated Chl-a values at point BF10 and BF13 except only one at BF10 station represented as dark orange line (19072018_G09_2B).

The second campaign was carried out on 10 September 2019. In this campaign, the amount of Chl-a at Lake Bafa is relatively low (Figure 6). All models were overestimated Chl-a values at all points. When both graphs are examined, M09 and NDCI models have significant similarities (light and dark blue lines in both figures) and they have close Chl-a value estimations.

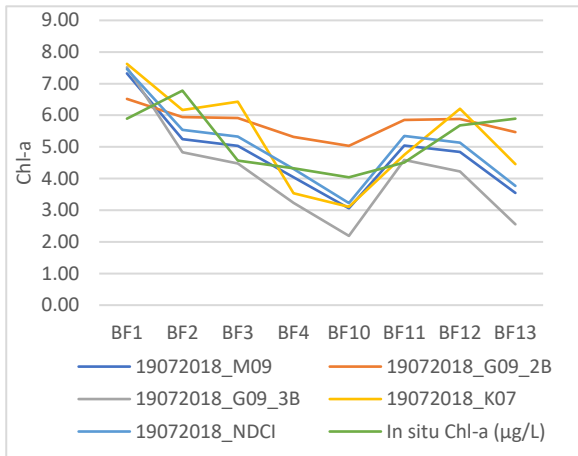


Figure 5. Chl-a values calculated from 19 July 2018 S2 image

Figure 7, 8, and 9 are the Chl-a distribution maps which obtained by applying selected algorithms to S2 images. The RGB band combinations of S2 images are B4-B3-B2 respectively. All thematic maps are

prepared with colors containing the same Chl-a range values.

We applied the algorithms to the S2 image dated 24 June 2018 to see the performance of the models at high Chl-a values during the algal bloom. As it is seen from the Figure 7 that the G09_2B model, which has the highest R^2 and the least error values, is insufficient to detect the high Chl-a values that occur during algal bloom.

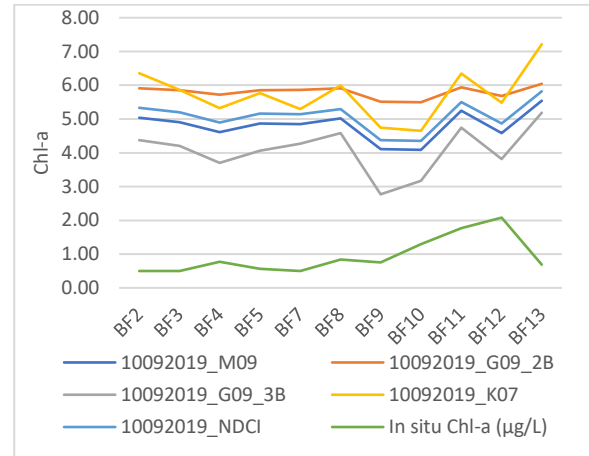


Figure 6. Chl-a values calculated from 10 September 2018 S2 image

The G09_2B model calculated the Chl-a value in the range of 5-10 $\mu\text{g/L}$ in the region where the algae bloom is intense (indicated with a red arrow as region a in Figure 7). The Chl-a value in the same region was calculated as 55-60 $\mu\text{g/L}$ by M09, 115-125 $\mu\text{g/L}$ by G09_3B, 35-40 $\mu\text{g/L}$ by K07, and 25-30 $\mu\text{g/L}$ by NDCI. All models calculated Chl-a values in the b region which is less affected by algal bloom in the range of 5-10 $\mu\text{g/L}$. It is clear from the thematic maps that models other than G09_2B predict the algal bloom pattern correctly.

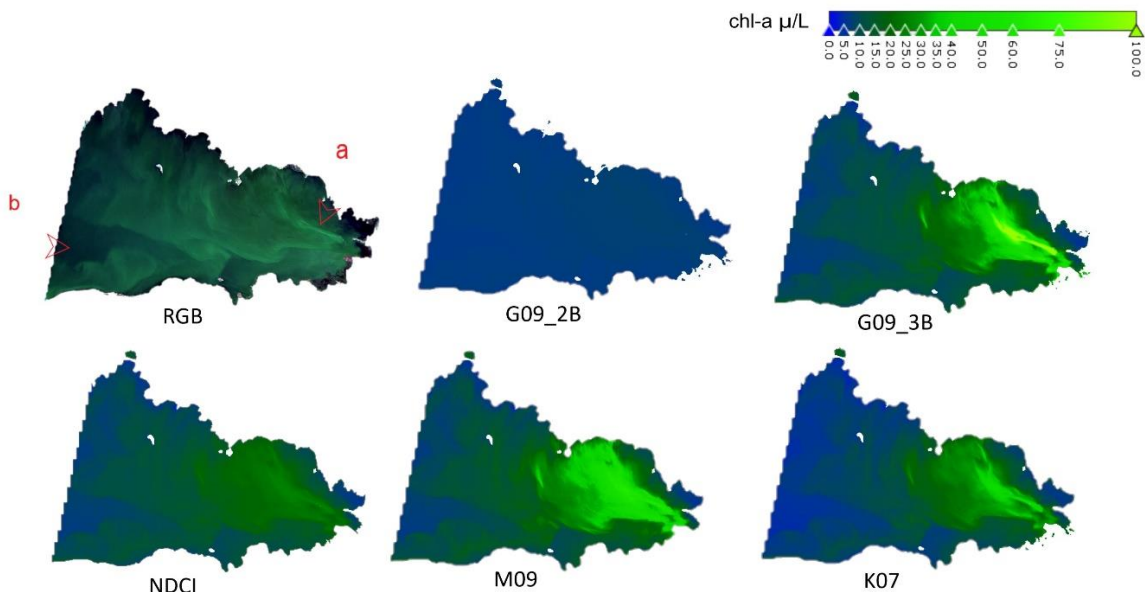


Figure 7. Chl-a distribution maps obtained by applying selected algorithms to S2 images on 24 June 2018.

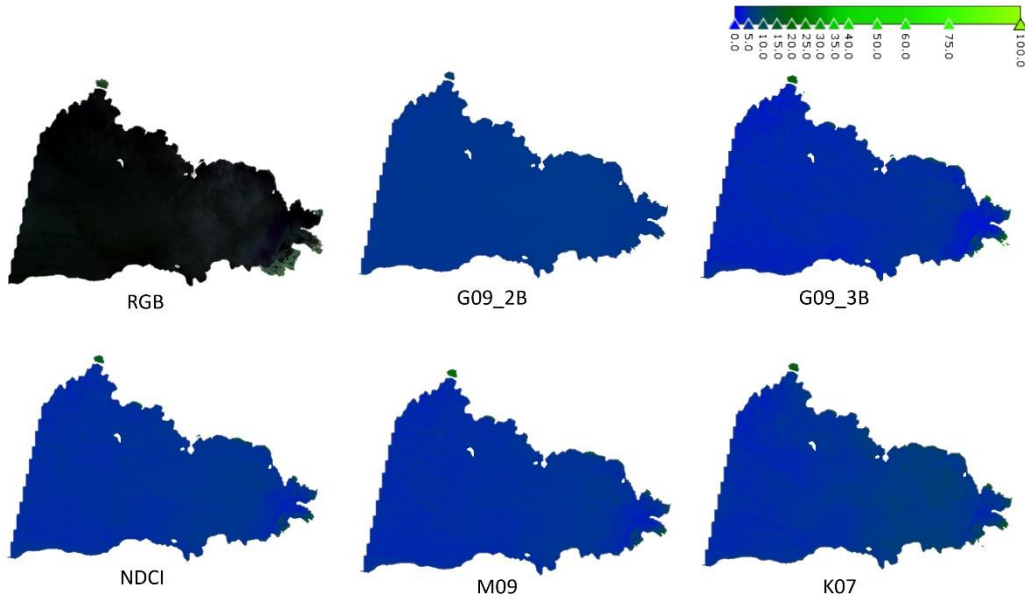


Figure 8. Chl-a distribution maps obtained by applying selected algorithms to S2 images on 19 July 2018

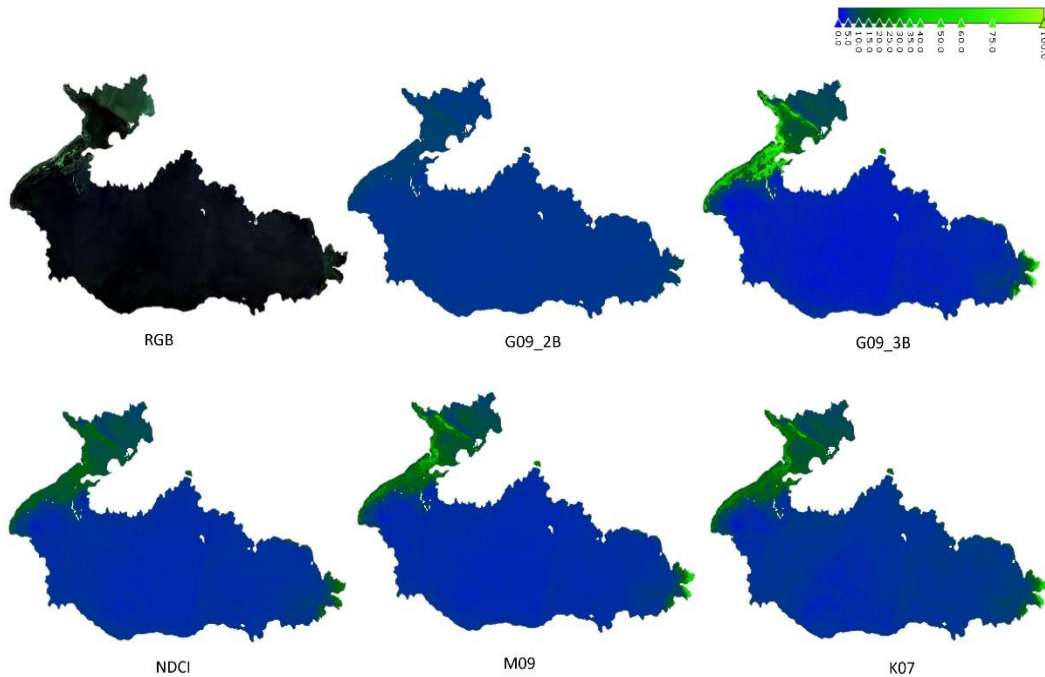


Figure 9. Chl-a distribution maps obtained by applying selected algorithms to S2 images on 10 September 2019

4. CONCLUSIONS

The performance of five commonly used and trending algorithms in estimating the Chl-a concentration in an inland water of Turkey has been investigated in this paper. The selected study area Lake Bafa is a productive lake and has a great potential for the performance test for the Chl-a estimation. 26 water samples constitute the in-situ data part of the study and they have been collected from 13 station points as two field campaigns. 20 reflectance spectra data have also been collected simultaneously and been used for simulating Sentinel 2 bands which constitutes the remotely sensed data part. The tested algorithms were selected according to their frequent use in the

literature about estimating Chl-a concentrations in inland and coastal water bodies.

For all algorithms, the R^2 , MSE, RMSE, %NRMSE, and MAPE values have been calculated. The R^2 values of M09, G09_2B, G09_3B, K07, and NDCI were calculated as 0.679, 0.749, 0.395, 0.726, and 0.7 respectively, so it can be said that there are significant correlations obtained for all algorithms.

According to analyses and research, although the G09_2B model had the best statistical results, it has failed in map validation process for high Chl-a values. The least correlation values have been calculated for Model G09_3B with the highest error values, and G09_3B and K07 tend to exaggerate the values.

When an algal bloom phenomenon occurs, high Chl-a concentration values may observe in any water body including inland and coastal areas. However, this is a phenomenon that happens only when optimum conditions exist. If the in-situ data collection date matches the algal bloom phenomenon, more information can be gained about the behavior, reliability, and accuracy of the algorithms. During the bloom that took place at the end of June and the beginning of July 2018 at the study area, it was not possible to collect in-situ data. Technical and organizational unexpected problems prevented this optimal match for this research as it is mentioned in previous sections of this paper.

As a conclusion, the M09 and NDCI models have a potential for Chl-a estimation in Lake Bafa since they provide better results. Both models had high R² and low error values and have similar results in analyses with S2 images. When the matching S2 image with the algal bloom was examined, both models were very successful in predicting the Chl-a pattern and they gave high concentration estimation values as they compared with the previous studies.

It is highly recommended for the future studies that, the Chl-a values can be estimated with higher accuracy when algorithms are calibrated with a data set containing a wider range of Chl-a values, in other words during the algal bloom phenomenon.

Acknowledgement

This research can be considered as a part of PhD Thesis of Elif Kirtiloglu with the title of "Evaluating Potential and Use of the Planet System in Terms of Detection, Monitoring, and Temporal Analysis of Cyanobacteria with Remote Sensing Techniques", Konya, Turkey, 2022.

This research was also supported by Konya Technical University Scientific Research Project (No 18201069).

Author Contributions

First Author: Conceptualization, Methodology, Software, Writing.

Second Author: Supervision, Methodology, Writing – Reviewing and Editing.

Conflicts of Interest

The authors declare no conflict of interest.

REFERENCES

- 10260 ISO. (1992). *Water quality measurement of biochemical parameters spectrometric determination of the chlorophyll-a concentration. International Organization for Standardization.*
- Beck, R., Xu, M., Zhan, S., Liu, H., Johansen, R. A., Tong, S., Yang, B., Shu, S., Wu, Q., Wang, S., Berling, K., Murray, A., Emery, E., Reif, M., Harwood, J., Young, J., Martin, M., Stillings, G., Stumpf, R., ... Huang, Y. (2017). *remote sensing Comparison of Satellite Reflectance Algorithms for Estimating Phycoyanin Values and Cyanobacterial Total Biovolume in a Temperate Reservoir Using Coincident Hyperspectral Aircraft Imagery and Dense Coincident Surface Observations.* 9, 538. <https://doi.org/10.3390/rs9060538>
- Falkowski, P. (2012). Ocean Science: The power of plankton. *Nature*, 483, 17–20. <https://doi.org/10.1038/483S17a>
- Field, C. B., Behrenfeld, M. J., Randerson, J. T., & Falkowski, P. (1998). Primary Production of the Biosphere: Integrating Terrestrial and Oceanic Components. *Science*, 281, 237–240. www.sciencemag.org
- Gitelson, A. A., Gurlin, D., Moses, W. J., & Barrow, T. (2009). A bio-optical algorithm for the remote estimation of the chlorophyll- a concentration in case 2 waters. *Environmental Research Letters*, 4(4), 45003. <https://doi.org/10.1088/1748-9326/4/4/045003>
- Hepsogutlu, D. (2012). *Macrobentic Organisms and Physicochemical Parameters of Bafa Lake (In Turkish)* [MSc Thesis]. Dokuz Eylul University.
- Hunter, P. D., Tyler, A. N., Carvalho, L., Codd, G. A., & Maberly, S. C. (2010). *Hyperspectral remote sensing of cyanobacterial pigments as indicators for cell populations and toxins in eutrophic lakes.* <https://doi.org/10.1016/j.rse.2010.06.006>
- Hunter, P. D., Tyler, A. N., Gilvear, D. J., & Willby, N. J. (2009). Using remote sensing to aid the assessment of human health risks from blooms of potentially toxic cyanobacteria. *Environmental Science and Technology*, 43(7), 2627–2633. <https://doi.org/10.1021/es802977u>
- Kesici, K. (2015). *The Research on the Factors that Causes Toxic Nodularia Spumigena Mertens ex Bornet & Flahault Blooms in Lake Bafa (In Turkish)* [PhD]. The Graduate School of Natural and Applied Science.
- Kızılkaya, I. T., Demirel, Z., Kesici, K., Kesici, E., & Sukatar, A. (2016). Morphological, Molecular and Toxicological Characterization of Nodularia spumigena Mertens in Jungens (1822) from Brackishwater Lake Bafa (Turkey). *Sinop Uni J Nat Sci*, 1, 39–52.
- Koçak, F., Aydın-Onen, S., Acik, S., & Kucuksezgin, F. (2017). Seasonal and spatial changes in water and sediment quality variables in Bafa Lake. *Environmental Earth Sciences*, 76. <https://doi.org/10.1007/s12665-017-6950-9>
- Koponen, S., Attila, J., Pulliainen, J., Kallio, K., Pyhäiähti, T., Lindfors, A., Rasmus, K., & Hallikainen, M. (2007). A case study of airborne and satellite remote sensing of a spring bloom event in the Gulf of Finland. *Continental Shelf Research*, 27, 228–244. <https://doi.org/10.1016/j.csr.2006.10.006>

- Kudela, R. M., Palacios, S. L., Austerberry, D. C., Accorsi, E. K., Guild, L. S., & Torres-Perez, J. (2015). Application of hyperspectral remote sensing to cyanobacterial blooms in inland waters. *Remote Sensing of Environment*, 167, 196–205.
<https://doi.org/10.1016/J.RSE.2015.01.025>
- Matthews, M. W., & Odermatt, D. (2015). Improved algorithm for routine monitoring of cyanobacteria and eutrophication in inland and near-coastal waters. *Remote Sensing of Environment*, 156, 374–382.
<https://doi.org/10.1016/j.rse.2014.10.010>
- Mishra, S., & Mishra, D. R. (2012). Normalized difference chlorophyll index: A novel model for remote estimation of chlorophyll-a concentration in turbid productive waters. *Remote Sensing of Environment*, 117, 394–406.
<https://doi.org/10.1016/j.rse.2011.10.016>
- Mishra, S., Mishra, D. R., Lee, Z., & Tucker, C. S. (2013). *Quantifying cyanobacterial phycocyanin concentration in turbid productive waters: A quasi-analytical approach.*
<https://doi.org/10.1016/j.rse.2013.02.004>
- Mobley, C. D. (1999). Estimation of the remote-sensing reflectance from above-surface measurements. *Applied Optics*, Vol. 38, Issue 36, Pp. 7442-7455, 38(36), 7442–7455.
<https://doi.org/10.1364/AO.38.007442>
- Moses, W. J., Saprygin, V., Gerasyuk, V., Povazhnyy, V., Berdnikov, S., & Gitelson, A. A. (2019). Olci-based nir-red models for estimating chlorophyll-a concentration in productive coastal waters—a preliminary evaluation. *Environmental Research Communications*, 1(1).
<https://doi.org/10.1088/2515-7620/aaf53c>
- Ozturk, Y. (2018). *Determination of Population Density and Propagation Map of Mytilaster Marioni (Locard, 1889) (Mollusca; Bivalvia; Mytilidae) in Lake Bafa (In Turkish).*
- Paerl, H. W., Hall, N. S., & Calandrino, E. S. (2011). *Controlling harmful cyanobacterial blooms in a world experiencing anthropogenic and climatic-induced change.*
<https://doi.org/10.1016/j.scitotenv.2011.02.001>
- Ruiz-Verdú, A., Simis, S. G. H., de Hoyos, C., Gons, H. J., & Peña-Martínez, R. (2008). *An evaluation of algorithms for the remote sensing of cyanobacterial biomass.*
<https://doi.org/10.1016/j.rse.2007.11.019>
- Shi, K., Zhang, Y., Li, Y., Li, L., Lv, H., & Liu, X. (2014). *Remote estimation of cyanobacteria-dominance in inland waters.*
<https://doi.org/10.1016/j.watres.2014.10.019>
- Soja-Wo, M., Craig, S. E., Kratzer, S., Wojtasiewicz, zena, Darecki, M., & Jones, C. T. (2017). *A Novel Statistical Approach for Ocean Colour Estimation of Inherent Optical Properties and Cyanobacteria Abundance in Optically Complex Waters.* 9, 343.
<https://doi.org/10.3390/rs9040343>
- Vinh, P. Q., Ha, N. T. T., Binh, N. T., Thang, N. N., Oanh, L. T., & Thao, N. T. P. (2019). Developing algorithm for estimating chlorophyll-a concentration in the Thac Ba Reservoir surface water using Landsat 8 Imagery. *VIETNAM JOURNAL OF EARTH SCIENCES*, 41(1), 10–20.
<https://doi.org/10.15625/0866-7187/41/1/13542>
- Watanabe, F., Alcântara, E., Rodrigues, T., Rotta, L., Bernardo, N., & Imai, N. (2018). Remote sensing of the chlorophyll-a based on OLI/Landsat-8 and MSI/Sentinel-2a (Barra Bonita Reservoir, Brazil). *Anais Da Academia Brasileira de Ciencias*, 90(2), 1987–2000.
<https://doi.org/10.1590/0001-3765201720170125>



© Author(s) 2021. This work is distributed under <https://creativecommons.org/licenses/by-sa/4.0/>